

Chapter 8

ACTIVATION MEASUREMENTS FOR THERMAL NEUTRONS

Part D. ^{36}Cl Measurements in the United States

Tore Straume, Alfredo A. Marchetti, Stephen D. Egbert, James A. Roberts, Ping Men, Shoichiro Fujita, Kiyoshi Shizuma, Masaharu Hoshi

Introduction

A large number of measurements were performed in the United States of ^{36}Cl in both granite and concrete samples obtained from various locations and distances in Hiroshima and Nagasaki. These measurements employed accelerator mass spectrometry (AMS) to quantify the number of atoms of ^{36}Cl per atom of total Cl in the sample. Results of these measurements are presented in this section and discussed in the context of the DS02 dosimetry reevaluation effort for Hiroshima and Nagasaki atomic-bomb survivors.

The production of ^{36}Cl by bomb neutrons in mineral samples from Hiroshima and Nagasaki was primarily via the reaction $^{35}\text{Cl}(n,\gamma)^{36}\text{Cl}$. This reaction has a substantial thermal neutron cross section (43.6 b at 0.025 eV), and the product has a long half-life (301,000 y). Hence, it is well suited for neutron-activation detection in Hiroshima and Nagasaki using AMS more than 50 years after the bombings. A less important reaction for bomb neutrons, $^{39}\text{K}(n,\alpha)^{36}\text{Cl}$, typically produces less than 10% of the ^{36}Cl in mineral samples such as granite and concrete, which contain ~2% potassium.

In 1988, only a year after the publication of the DS86 final report (Roesch 1987), it was demonstrated experimentally that ^{36}Cl measured using AMS should be able to detect the thermal neutron fluences at the large distances most relevant to the atomic-bomb survivor dosimetry (Straume et al. 1990). Subsequent measurements in mineral samples from both Hiroshima (Straume et al. 1992) and Nagasaki (Straume et al. 1994) validated the experimental findings. The potential utility of ^{36}Cl as a thermal neutron detector in Hiroshima was first presented by Haberstock et al. (1986) who employed the Munich AMS facility to measure $^{36}\text{Cl}/\text{Cl}$ ratios in a gravestone from near the hypocenter. That work subsequently resulted in an expanded ^{36}Cl effort

in Germany (see Chapter 8, Part E) that paralleled the U.S. work. More recently, there have also been ^{36}Cl measurements made by a Japanese group (see Chapter 8, Part F).

The impetus for the extensive ^{36}Cl and other neutron activation measurements was the recognized need to validate the neutron component of the dose in Hiroshima. Although this was suggested at the time of the DS86 Final Report (Roesch 1987), where it was stated that the calculated neutron doses for survivors could possibly be wrong, the paucity of neutron validation measurements available at that time prevented adequate resolution of this matter. It was not until additional measurements and data evaluations were made (e.g., Straume et al. 1992; Shizuma et al. 1993) that it became clear that more work was required to better understand the discrepancies observed for thermal neutrons in Hiroshima. This resulted in a large number of additional neutron activation measurements in samples from Hiroshima and Nagasaki by scientists in the U.S., Japan, and Germany. The results presented here for ^{36}Cl , together with measurements made by other scientists and for other isotopes (see Chapters 8 and 9 of this report), now provide a much improved measurement basis for the validation of neutrons in Hiroshima.

^{36}Cl Measurements in Samples from Hiroshima

Materials and Methods

Samples. Mineral samples from many distances in Hiroshima were measured for ^{36}Cl in the present study. Table A1 of Appendix A gives the sample locations and also identifies the sample material and distance from the hypocenter. Here, DS86 and DS02 ground ranges are distances from the respective hypocenters to the sample locations based on the new city map and aerial photos (see Chapter 5). Samples include both granite and concrete, and were obtained as both near-surface samples and deep cores. It is also noted that the sample locations span the most significant distances for atomic-bomb survivor dosimetry, i.e., from near the hypocenter to more than 2 km, and are spaced to provide good coverage of measurement results throughout this range.

The measurements in near-surface granite samples are used to provide line-of-sight comparisons with DS86 and DS02 calculations as a function of distance from the bomb hypocenter. The ^{36}Cl depth profiles in cores provide a more stringent test of the sample modeling calculations. That is, if the measurement and calculation agree at the surface but not at depth, a possible implication would be that the calculation is not accounting sufficiently for the sample environment, e.g., elemental composition, water content, etc. In contrast, agreement at depth but not at the surface could suggest surface alterations (such as adding surface cement or tiles) or chloride surface exchange (chloride is highly mobile especially in porous materials such as cement and could potentially affect the $^{36}\text{Cl}/\text{Cl}$ ratio near the surface). Taken together, these approaches are used to provide a good thermal neutron measurement basis against which the dosimetry calculations can be tested.

Overall, these samples have provided a large number of ^{36}Cl measurements, and the results are listed in Tables A2-A14 of Appendix A. The results also include measurements in granite samples selected for intercomparison between the ^{36}Cl and ^{152}Eu measurement groups (Table A13 of Appendix A), as well as measurements of solutions of Cl and Eu irradiated with neutrons in the laboratory to evaluate relative responses of the reactions $^{35}\text{Cl}(n,\gamma)^{36}\text{Cl}$ and $^{151}\text{Eu}(n,\gamma)^{152}\text{Eu}$ to thermal and epithermal neutrons (see Chapter 8, Part H).

Elemental Analysis of Samples. Selected samples were analyzed to provide information on the elemental compositions of the materials used in the present study. Of particular concern was the potential heterogeneity of concretes. Extensive elemental analyses were therefore performed on several concrete cores from different sampling locations in both Hiroshima and Nagasaki. The compositions of both trace elements and major minerals for concrete cores are listed in Tables A15 and A16 of Appendix A. It is observed that the compositions among the concrete cores obtained from various locations in Hiroshima are similar. Inter-core differences are generally less than a factor of two for most elements.

Also of concern was the possibility that trace elements with high neutron cross sections, such as gadolinium (Gd), cadmium (Cd), and boron (B), may significantly affect the thermal neutron fluence in the samples and surrounding materials. Those elements were therefore measured in four representative concrete cores using high precision methods. The concentrations of Gd, Cd, B, and Li are listed in Table A17 of Appendix A for concrete cores from the Gokoku Shrine, the Hiroshima Kirin Beer Hall, the old Hiroshima City Hall, and the Hiroshima University Elementary School. It is observed that Gd, Cd, and B in the four cores differ by less than a factor of two. For the sample-specific DS02 and DS86 calculations, a nominal constant value was assumed for poisons (see Chapter 8, Part J). The elemental composition measurements would suggest the following maximum uncertainties in the calculated $^{36}\text{Cl}/\text{Cl}$ ratios in these samples: 2% at the surface, 5% at 5 cm, 7.5% at 10 cm, 12.5% at 20 cm, and 15% at 30 cm.

Sample Preparation. The cores were typically cut into 2-to-3 cm thick slices. For concrete cores, the first slice usually contained the cement-like material (and in some cases, tiles) on the outside of the wall. Concrete was usually reinforced with steel rods. This sometimes affected the thickness of the slice as well as which slices were most suitable for ^{36}Cl measurement. Because of the possibility of surface chloride exchange, surface contamination, or resurfacing of the building after the war, the surface cement (typically, a few cm depth) of the concrete core is considered unreliable for the determination of bomb-induced ^{36}Cl activation.

The concrete slices were ground using a dedicated Shatter Box to >200 mesh (<125 μm) and leached in 50-g batches to extract chlorides from the sample (1:5, weight sample per weight solvent). Two extraction methods were employed, and both were described in Straume et al. 1994. Prior to 1994, the chloride was extracted from the ground sample by distillation in concentrated hydrofluoric and nitric acids. This method was adopted from those generally employed in rock dating (Elmore and Phillips 1987). The principal advantage of the distillation method is that it may, depending on the sample material and processing procedures used, permit the separation of *in situ* chloride (i.e., bomb-induced plus cosmic-ray induced) from chloride that may have been introduced by meteoric contamination. The disadvantage is that large amounts of concentrated acids must be used, resulting in risk to laboratory workers as well as significant amounts of hazardous wastes. In 1994, we tested whether it was necessary to use concentrated acids to extract chloride from the samples. Results from distillation in concentrated acids were compared with same-sample results using only deionized water leaching. The results, reported in Straume et al. (1994), demonstrated that, when surface cement was not included, there was very little difference between the two extraction methods in concretes. Hence, the concentrated acid distillation extraction method has not been employed since 1994.

Accelerator Mass Spectrometry. The measurements reported here were made using three AMS facilities: the Center for Accelerator Mass Spectrometry (CAMS) at the Lawrence Livermore National Laboratory, the PRIME Lab at Purdue University, and the AMS facility at the University of Rochester, NY. Each of these facilities has a typical detection limit of a few atoms of ^{36}Cl per 10^{15} atoms of Cl (Elmore and Phillips 1987). The measured $^{36}\text{Cl}/\text{Cl}$ ratios are normalized with respect to standards from the National Institute of Standards and Technology. The standards used at both Lawrence Livermore National Laboratory (LLNL) and Purdue were from NIST 4943 SRM, a dilution prefixed KN and referenced in Sharma et al. 1990. Analytical precision of ~3 to 5% are typical for ^{36}Cl using AMS.

Calculations for Hiroshima. The calculations of the activation of ^{36}Cl in concrete and granite samples were performed using the Monte Carlo Adjoint Shielding Code System (Johnson 1999). This is the same methodology used for both DS86 and DS02. The code is ideal for situations in which a shielded detector point is exposed to a large field of incident neutrons or gamma rays. Neutrons are started at the point of measurement *in situ* and run backwards in space and time to exit a closed surface that surrounds the sample and shield. A further discussion of this code and the calculations is found in Chapter 8, Part J.

Geometry Model. The shielding around the measurement location is modeled using a combination of primitive bodies, like boxes and ellipsoids. For each of the calculations, geometric models consisting of about ten primitive bodies were used. The important aspects of the geometry are the sample height and depth in the material. For thermal neutron activation, and to a lesser extent for fast neutron activation, it is important that nearby structures not in the line-of-sight be included.

Materials. The building and sample elemental compositions (especially hydrogen content) are important in the calculation. The materials chosen for the calculations are specific to the building. If the elemental constituents were measured for the sample, then those constituents were used in the calculations. If the sample constituents were not measured, representative compositions were used, taking into account the type of material. When trace elements are unknown, a representative amount was assumed for the material.

Transport Cross Sections. The neutrons were transported through the materials using ENDF/B6.2 cross sections in DABL-69 group format (Ingersoll et al. 1989; McVane et al. 1995; White et al. 2000). Some of the key trace elements are not included in this cross-section library, such as gadolinium and samarium. Their contributions to the absorption cross sections were accounted for by adding an amount of cadmium necessary to produce the same absorption cross section. Cadmium was chosen because its thermal-to-epithermal absorption cross-section ratio is similar to those of the key trace elements.

Fluences. The unperturbed air-over-ground neutron fluences were obtained from discrete ordinate calculations of both the prompt and delayed neutron sources as described in Chapter 3.

Responses. The $^{35}\text{Cl}(n,\gamma)^{36}\text{Cl}$ and $^{39}\text{K}(n,\alpha)^{36}\text{Cl}$ neutron responses were derived from ENDF/B6.2. They were converted from fine multipoint data to the DABL-69 group structure by collapsing with representative spectra 1 meter above ground at Hiroshima. There is some uncertainty about the thermal portion of the $^{39}\text{K}(n,\alpha)^{36}\text{Cl}$ reaction. It does not appear to be well established. However, it does not contribute much to activation for the A-bomb fluences. The potential implications of this on the calculations are discussed in Chapter 8, Part J.

Coupling. Each neutron that reaches the closed surface was multiplied by the neutron fluence

according to its energy and angle. This represents the activation to the point of measurement. The contributions from all the neutrons were averaged.

Results. The results from the DS86 and DS02 sample-specific modeling calculations are presented here together with the measurement data. The fast-neutron reaction $^{39}\text{K}(n,\alpha)^{36}\text{Cl}$ is a small portion of the total activation until the farther distances at Hiroshima. For example, it contributes less than 1% of the activation at distances within 400 m from the hypocenter. However, beyond 1,000 m it can account for ~10%, depending on the shielding and potassium concentration in the sample. This is due to the rapid and continual hardening of the Hiroshima neutron spectrum during air transport. The calculations of ^{36}Cl production include activation from fast and thermal neutrons and from prompt and delayed neutrons, and for both the $^{35}\text{Cl}(n,\gamma)^{36}\text{Cl}$ and $^{39}\text{K}(n,\alpha)^{36}\text{Cl}$ reactions.

Hiroshima Results and Discussion

Background for ^{36}Cl in Granite and Concrete

Background becomes a significant issue for ^{36}Cl at distances beyond about 1,200 m ground range. This is because of the long half-life of ^{36}Cl (301,000 years), which permits readily measurable ^{36}Cl in the earth's surface as well as the possibility that long-lasting contamination may occur from man-made sources of ^{36}Cl . The significant isobar for ^{36}Cl is ^{36}S . High concentration of sulfur can reduce the precision of the ^{36}Cl measurement, and occasionally, even prevent the measurement of ^{36}Cl in some samples. Mineral samples may contain quite different concentrations of sulfur. Our findings have been that the heterogeneous nature of concretes results in a broader range of sulfur concentrations than in granites. For example, none of the granite samples measured for ^{36}Cl in the present study was too high to measure due to their sulfur concentrations, whereas, some of the concrete samples were problematic due to high sulfur.

Various approaches have been pursued to better define the ^{36}Cl background of the kinds of samples measured in these dosimetry evaluations. One approach has been to measure core profiles to determine the background directly in the same material. Another approach has been to measure samples of the same kind, either highly shielded from the same building or at large distances from the bomb explosions where significant neutron exposure did not occur. For granite samples, yet another approach has been employed to find unexposed granites of similar history as the exposed ones, i.e., same rock quarry, depth, etc. (see Chapter 8, Part E).

For granites, a number of background measurements have now been made in samples from Hiroshima (Chapter 8, Parts E and F, and this section). For samples not exposed significantly to bomb neutrons, the $^{36}\text{Cl}/\text{Cl}$ ratios tend to be in the 1 to 2×10^{-13} range, similar to those generally observed in deep concretes (see below).

For concretes, background measurements have been made in samples from both Hiroshima and Nagasaki. These background measurements were in samples that were either heavily shielded or at large distances, where the contribution from bomb neutrons was small. Also, the background in deep concrete cores and in surface cement has been evaluated. Results from the background measurements in deep concrete cores (i.e., where potential surface contamination from meteoric sources would be unlikely) are plotted in Figure 1 and show $^{36}\text{Cl}/\text{Cl}$ ratios on the order of 10^{-13} . The values range between 0.8 and 1.8×10^{-13} . The mean ratio of the measurements is 1.24×10^{-13} and the standard deviation (SD) is 0.30×10^{-13} . A feature of the background measurements in deep concrete cores is the use of relatively large sample sizes. Typically, about

500 g of concrete are ground to a fine powder and mixed well to provide an average $^{36}\text{Cl}/\text{Cl}$ ratio that would presumably be fairly representative of the concrete wall.

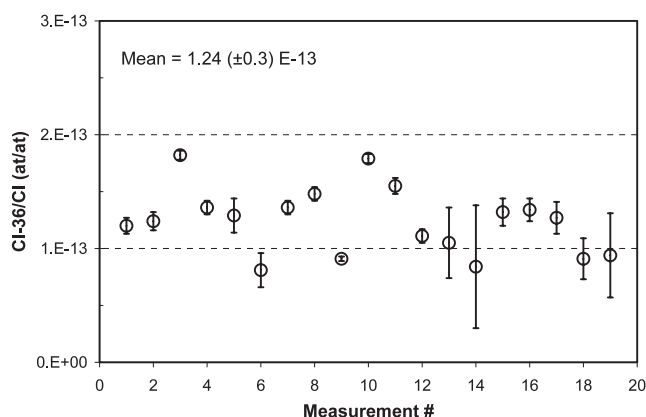


Figure 1. Background of $^{36}\text{Cl}/\text{Cl}$ measured in concrete from Hiroshima and Nagasaki. Measurements were in deep concrete cores, i.e., no surface cement.

In contrast, measurements in surface cement from a variety of concretes from Hiroshima and Nagasaki show that the “background” $^{36}\text{Cl}/\text{Cl}$ ratios tend to be more variable than those measured deeper in the cores. The results available show that $^{36}\text{Cl}/\text{Cl}$ ratios in surface cement from Hiroshima and Nagasaki typically fall within the range 1×10^{-13} to 4×10^{-13} , occasionally even higher, and tend to scatter more than those observed in deep concrete. The differences observed between background $^{36}\text{Cl}/\text{Cl}$ in deep concrete and surface cement may reflect the different sources of materials (i.e., surface cement is applied later and not part of the original concrete wall) and possible surface contamination from meteoric and other external sources of chloride.

In this connection, it may be important to note that $^{36}\text{Cl}/\text{Cl}$ ratios measured in rain water in the northern hemisphere during the 1950s and early 1960s were more than 1,000 times higher than they are today (Schaeffer et al. 1960; Elmore et al. 1982; Synal et al. 1990). The reason for this was the very large amounts of ^{36}Cl injected into the atmosphere by nuclear bomb tests at that time, apparently associated with the neutron irradiation of sea water (Schaeffer et al. 1960; Phillips 1999). This is strongly suggested by the detailed measurements of ^{36}Cl deposition performed on the Dye-3 ice core from Greenland by Synal et al. (1990). Those measurements indicate that major ^{36}Cl fallout began in 1954 and coincides with the timing of events Romeo (11 Mt), Union (6.9 Mt), and Yankee (13.5 Mt) in April and May of 1954, which were the first thermonuclear explosions on barges (Phillips 1999). Most of the neutrons released by previous thermonuclear explosions on atolls were absorbed by rock, resulting in little activation of seawater (Zerle et al. 1997). From 1956 through 1958 there were 32 additional barge explosions totaling 30.4 Mt. It has been reported that these tests were apparently responsible for nearly all stratospheric injection of ^{36}Cl and that approximately 17% of the released neutrons were absorbed by ^{35}Cl in seawater (Zerle et al. 1997; Phillips 1999).

An example of the ^{36}Cl bomb pulse is illustrated in Table A18 of Appendix A, where ^{36}Cl measurements were made in rain water collected in New York. Similar ^{36}Cl levels were detected in other parts of the northern hemisphere during that time period (e.g., Elmore et al. 1982; Synal et al. 1990; and a recent review by Phillips 1999). The substantial body of bomb-pulse data now available for ^{36}Cl indicates a maximum at mid-northern latitudes when corrected for amount of precipitation (Phillips 1999). Although we are not aware of ^{36}Cl bomb-pulse precipitation data reported from Hiroshima, the data in Phillips (1999) together with precipitation data from Hiroshima (about 155 cm per year, ~ 34 degrees north latitude) would suggest that the ^{36}Cl in Hiroshima rain water during the late 1950s and early 1960s should have been similar to that observed in New York, which has about 127 cm precipitation per year and is about 41 degrees north latitude. Of course, it is recognized that the high concentrations in rain would be substantially diluted with chloride in surface concrete, perhaps to the background levels that are now observed in surface cement.

It should be added that the potential for surface problems in concrete (including "background" problems) was recognized in 1993, when the first ^{36}Cl measurements were made in cores from Nagasaki (Straume et al. 1994). An attempt was made in that study to avoid such potential problems by selecting samples from inside the reinforced concrete wall itself, beginning typically at a few centimeters depth from the outside surface of the wall. Subsequent to 1994, our measurements of ^{36}Cl depth profiles in many cores, both concrete and granite, have provided a better understanding of ^{36}Cl at the surface and at depth, and have demonstrated that the unexpectedly high surface measurements at large distances (Straume et al. 1992) were not produced by bomb neutrons. Rather, those results were associated with a surface phenomenon particularly noticeable in cement.

Overall, a nominal background of $1.24 (\pm 0.30) \times 10^{-13} \text{ }^{36}\text{Cl}/\text{Cl}$, obtained from Figure 1, has been subtracted from all the measurements in this section (both granite and concrete) to provide estimates of the bomb-induced neutron activation, which are then compared with sample-specific calculations. It is noted that this nominal background, although generally consistent with average backgrounds for granites and deep concretes in Hiroshima, may not be strictly correct for a particular sample. This is illustrated by the variations in ^{36}Cl measured in core profiles at large distances, where bomb neutrons do not contribute significantly to the ^{36}Cl production.

^{36}Cl Activation vs Distance in Hiroshima

Line-of-Sight Granite Samples. The measurement results for ^{36}Cl in surface granite in line-of-sight with the bomb explosion are plotted in Figure 2. Ground range is the distance from the hypocenter (the point on the ground directly under the bomb explosion) to the sample. The DS02 sample-specific modeling calculations are also plotted for comparison.

It is clear that the measurements and DS02 calculations for near-surface granite samples agree well at the distances evaluated. This agreement holds even if a background for $^{36}\text{Cl}/\text{Cl}$ is not subtracted from these measurements, as seen in Figure 3. Comparing the results in Figures 2 and 3 illustrates that uncertainties in the background for ^{36}Cl in these granite samples should not have a significant effect on the measurement-to-calculation comparisons within 1,000 m from the hypocenter.

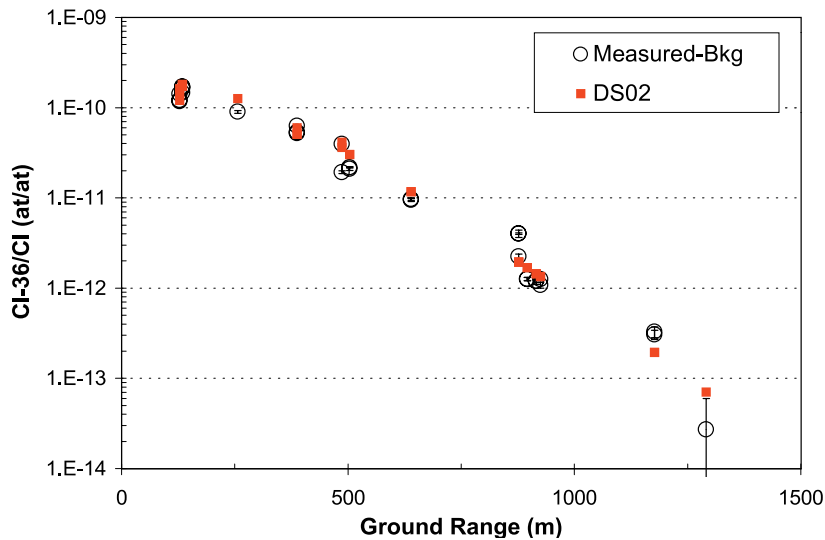


Figure 2. Comparison of measured and DS02 calculated ^{36}Cl in near-surface granite samples from Hiroshima. A nominal background of 1.24×10^{-13} $^{36}\text{Cl}/\text{Cl}$ was subtracted.

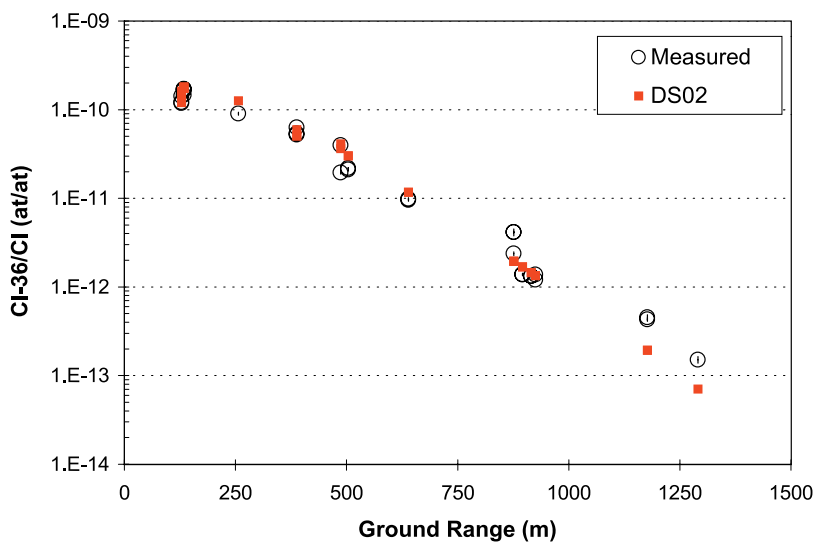


Figure 3. Comparison of measured and DS02 calculated ^{36}Cl in near-surface granite samples from Hiroshima. Background $^{36}\text{Cl}/\text{Cl}$ not subtracted.

When the ^{36}Cl measurements are compared with sample-specific DS86 calculations, agreement is also observed (Figure 4). It should be noted that the calculated 14% difference between DS86 and DS02 is not detectable by the measurements in Figures 2 and 4. It should also be noted that the ground ranges of the data points are slightly different for DS86 than those used with DS02. This is because both the hypocenter and sample locations were reevaluated for DS02, which changed sample distances somewhat compared with those employed in DS86.

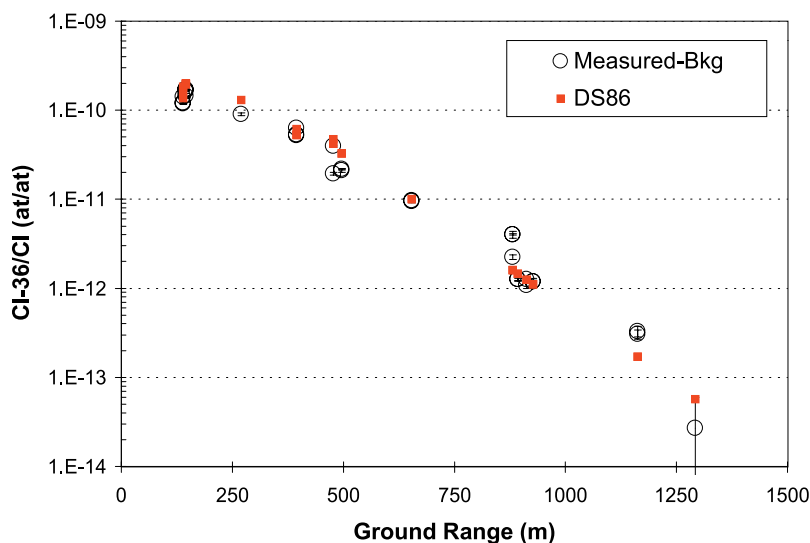


Figure 4. Comparison of measured and DS86 calculated ^{36}Cl in near-surface granite samples from Hiroshima. Background of 1.24×10^{-13} $^{36}\text{Cl}/\text{Cl}$ was subtracted.

If we divide the $^{36}\text{Cl}/\text{Cl}$ measured in the line-of-sight granite samples by the results from the sample-specific DS02 calculations, measured-to-calculated ratios are obtained as seen in Figure 5. The arithmetic mean M/C for the entire data set is 1.0 ± 0.4 , and the weighted mean is 0.9 ± 0.4 , neither is significantly different from unity. As pointed out above, it should also be noted that the M/C ratios within 1,000 m are not likely to be affected substantially by uncertainties in the background for $^{36}\text{Cl}/\text{Cl}$.

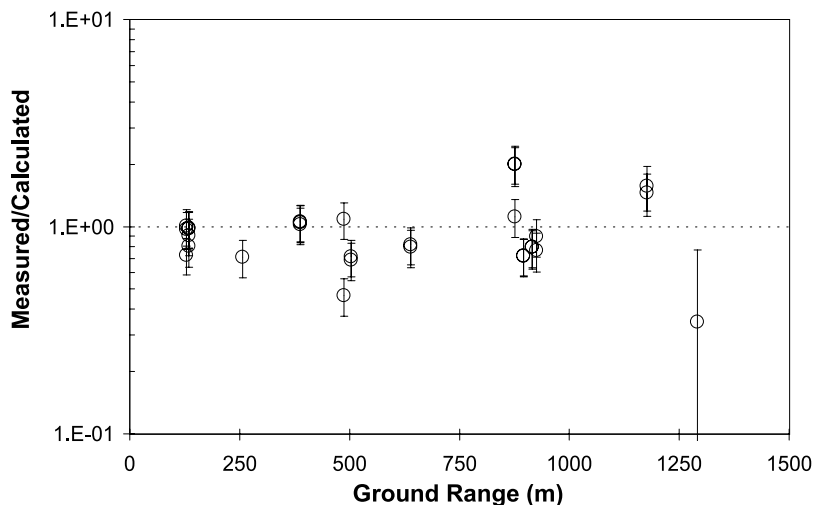


Figure 5. Measured-to-calculated ratios obtained for ^{36}Cl in Hiroshima. The measurements are for the near-surface granite samples in Figures 2 to 4, and the sample-specific calculations are for DS02.

Measurements in Concrete Samples. Measurements of ^{36}Cl in concrete samples have also been made in Hiroshima. The $^{36}\text{Cl}/\text{Cl}$ profiles for a number of concrete cores have been measured and compared with sample-specific calculations. A few of the surface cement samples measured for ^{36}Cl were not part of the cores described below. For completeness, those data are listed in Table A14, and include results for two samples previously presented in Straume et al. (1992). Due to factors such as possible modification of the surface after the war and the porous nature of concrete allowing entrance and potential exchange of chloride at the surface, we believe that surface concrete is less reliable than surface granite for line-of-sight neutron dosimetry.

Examples of surface modifications that can affect the measurement results in Hiroshima concretes are illustrated by the core profiles discussed below. It should be noted, however, that although concrete is more likely to have potential surface problems than granite, bomb-exposed concrete has been easier to obtain than granite from Hiroshima and Nagasaki. This is particularly the case for cores. Also, the study of core profiles goes beyond the surface issues and can provide important and reliable comparisons at depth. It is also noted that the ingredients of concrete (excluding the surface cement, which was applied later), although heterogeneous, were well mixed at the time of construction, which should have eliminated any cosmic-ray profile that could potentially be present in granite formations. Cosmic-ray profiles for $^{36}\text{Cl}/\text{Cl}$ in rock formations at the surface of the earth are illustrated in Dep et al. (1994) for various rock types and water concentrations. Their finding was that the cosmic-ray production of ^{36}Cl could result in a factor of two change in the $^{36}\text{Cl}/\text{Cl}$ ratio within the first meter of the rock surface.

The porous nature of cement, allowing chloride penetration from rain and other environmental sources, is supported by data illustrating that chloride in concrete can be transferred from the surface to several cm depth. For example, the use of salt for deicing of concrete-surfaced bridges has been studied extensively because of the concern that if the salt

penetrates into the steel infrastructure, the bridge can be damaged through increased rate of oxidation. Results from Paulsson-Tralla and Silfwerbrand (2002) indicate that the chloride deposited on the concrete surface of bridges can penetrate to several cm, and that the spring and summer rains can wash out much of the added Cl because of the lower chloride concentration in the rainwater than in the concrete. This shows that Cl is quite mobile in concrete and can seasonally wash in and out of the surface cement.

It is also noteworthy that total Cl concentration may be increased near the surface of concrete, but apparently not near the surface of granite. This is illustrated by the total Cl profiles measured in concrete and granite cores. Examples of concrete and granite core profiles measured for total Cl concentration are shown in Figures 6 and 7. The concrete core profiles illustrated in Figure 6 are from the Red Cross Hospital. It is clear that the ppm Cl is much higher at the surface than deeper in the concrete wall. This high level of Cl in the surface of the concrete may suggest Cl contamination from meteoric sources, perhaps mixed with aerosolized sea water. It is also possible that the high Cl concentration near the concrete surface could be caused, at least in part, by higher levels of Cl inherent in the surface cement, which is different from the concrete. For example, the surface cement may include local river water, which may be mixed with sea water and therefore also be high in Cl content. It should be noted that there could potentially be less restrictions on the salinity of the water used in surface cement than in concrete, because there are no rebars in the surface cement. Also, the surface cement does not contain coarse gravel, which may be mined and thus shielded from cosmic rays.

In contrast to the total Cl measured in concrete, the results for granite cores do not appear to show such profiles. The total Cl concentrations measured in granite cores obtained from the Shirakami shrine and Motoyasu bridge are seen in Figure 7. It is observed that the total Cl concentration is essentially constant at all depths through the cores. Particularly noteworthy is the observation that there is no increased Cl at the exposed surface of the granite cores.

In summary, the surface effect associated with ^{36}Cl measurements in cement is illustrated by the M/C ratios in Table A14 of Appendix A, where the measurements in surface cement are lower than the calculations near the hypocenter and become larger than the calculations beyond about 1,300 m when subtracting a nominal background for deep concrete. These results are consistent with meteoric dilution of bomb-induced ^{36}Cl near the hypocenter, and a higher ^{36}Cl “background” in surface cement than in deep concrete, which becomes evident only at large distances, where bomb-induced ^{36}Cl is negligible.

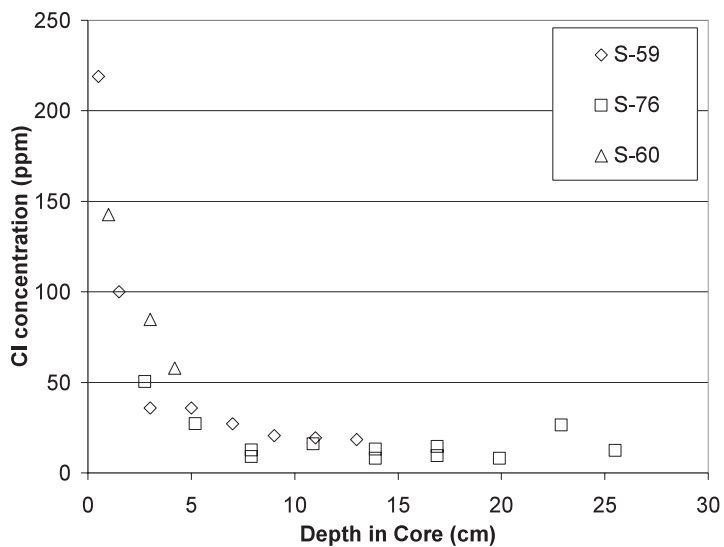


Figure 6. Total Cl measured in concrete cores. The concrete cores (S-59, S-60, and S-76) are from the Red Cross Hospital in Hiroshima.

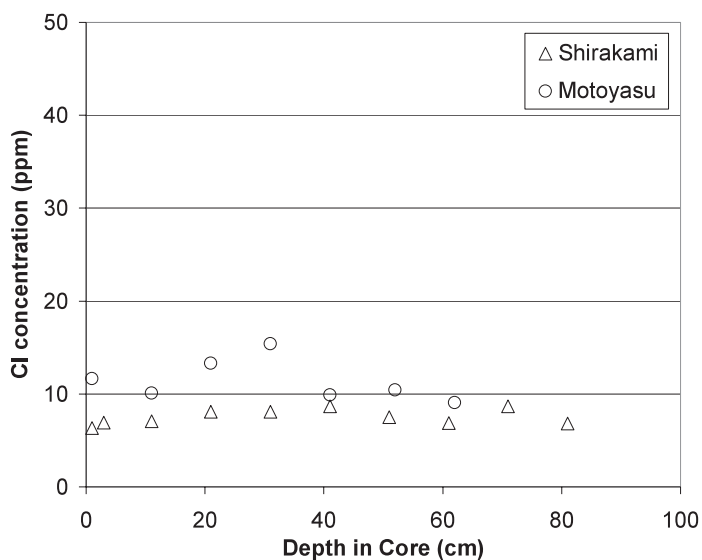


Figure 7. Total Cl measured in granite cores. The granite cores are from the Shirakami Shrine and the Motoyasu Bridge in Hiroshima.

Core Depth Profiles for ^{36}Cl

Depth profiles of ^{36}Cl measured and calculated in granite and concrete cores are presented and discussed below. These depth profiles provide a stringent test for the sample-specific calculations and illustrate the many complexities associated with reconstructing the precise environment in and around a sample location more than half a century later.

It is noted that concrete cores generally contained steel reinforcement bars, which could potentially have some effect on the thermal neutron fluence in a particular slice. Due to the complexity of many and varied steel bars, they were not included in the modeling calculations. Of course, granite cores did not include steel bars and would therefore avoid that added complexity. The positions and the thickness of the slices in concrete cores were determined to some extent by the locations of the steel bars.

Motoyasu Bridge (granite core, ~130 m from hypocenter). The ^{36}Cl measurement results are plotted in Figure 8 together with the sample-specific DS86 and DS02 calculations. The DS86 calculations appear to be consistently higher than the measurements at all depths in the core. In contrast, the DS02 calculations are essentially indistinguishable from the measurements. Given the complexity of both the measurements and the calculations, the agreement is outstanding. Note that the third depth point from the surface was from the bridge railing while the others were from the bridge pillar. The difference in geometry resulted in both the measurements and the calculations being somewhat higher at that point. The first four measurements in Table A3 are repeat measurements of the surface slice (0 to 2 cm depth) and of a slice cut from 3 to 5 cm depth. The weighted mean results for the surface slice is 1.63×10^{-10} (SD, 8.65×10^{-12}) and for the deeper slice is 1.70×10^{-10} (SD, 2.84×10^{-12}). These do not differ significantly, indicating that there was not a detectable surface effect in this particular granite sample.

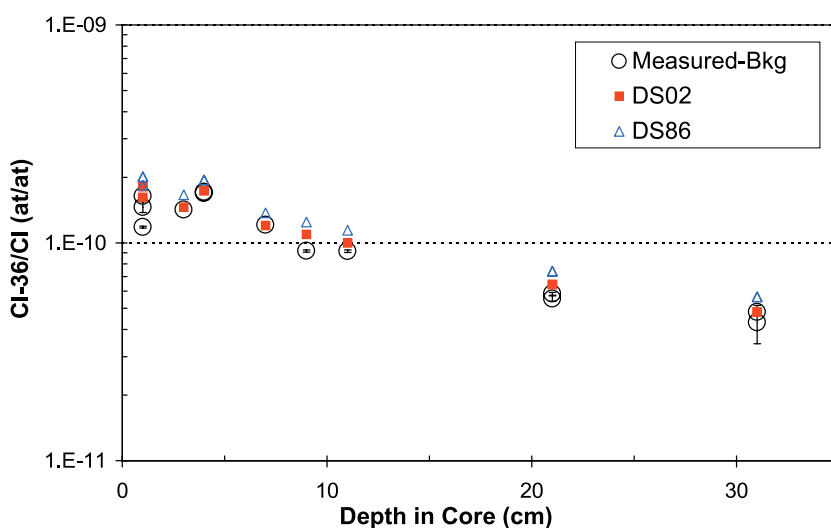


Figure 8. Depth profile in granite core from the Motoyasu Bridge in Hiroshima. Measurements are compared with DS02 and DS86 sample-specific calculations.

Gokoku Shrine Torii Gate (concrete footing and granite collar, 388 m from hypocenter).

The ^{36}Cl measurements in these samples are plotted in Figure 9 together with the sample-specific DS86 and DS02 calculations. Several observations are noteworthy. First, the $^{36}\text{Cl}/\text{Cl}$ ratios measured near the surface are substantially lower in the concrete than in the granite, even though both of these samples are in essentially the same location, i.e., the concrete was the in-ground footing and the granite collar was sitting directly on top of the footing but not shielding the location where the concrete core was taken. These results may suggest that the lower $^{36}\text{Cl}/\text{Cl}$ ratios in the surface concrete results from more chloride exchange in the porous concrete than in the much less penetrable granite. It is noted that modern rain water has typical $^{36}\text{Cl}/\text{Cl}$ ratios in the 5×10^{-14} to 1×10^{-13} range near the coast at mid-northern latitudes (Hainsworth et al. 1994) and therefore would tend to reduce the $^{36}\text{Cl}/\text{Cl}$ ratios measured in porous surface samples at distances less than about 1 km in Hiroshima, if the rainwater chloride had exchanged with or otherwise diluted the chloride in the surface cement. This would be consistent with the observation that the $^{36}\text{Cl}/\text{Cl}$ measured in the granite collar are in much better agreement with calculations. However, neither DS02 nor DS86 calculations agree with the measurements at depth in the concrete core, although the slopes are similar.

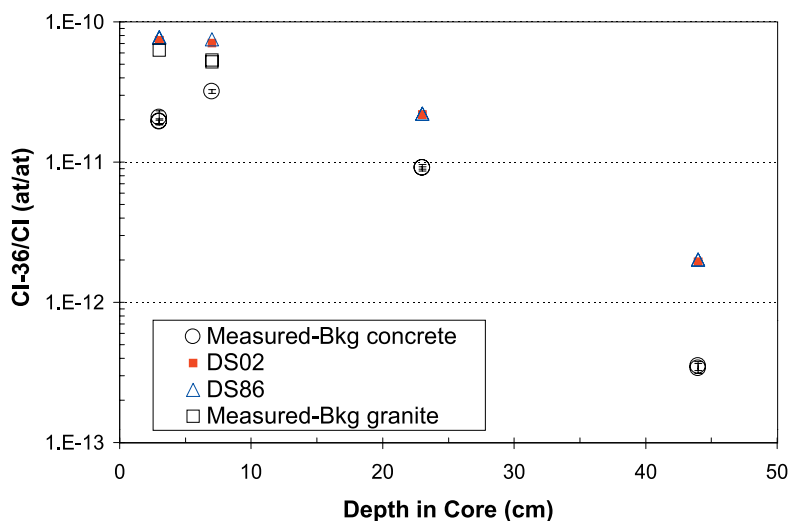


Figure 9. Depth profile in concrete and granite cores from the Gokoku Shrine in Hiroshima.

It is not expected that chloride surface exchange can significantly penetrate to such large depths in concrete (i.e., 22 cm and 45 cm), and therefore the discrepancy at these depths must have another cause. This conclusion is supported by the observation that measurements of ^{152}Eu in this same concrete core (Shizuma et al. 1997) are also lower than predicted by DS86 and DS02 calculations. It is possible, even likely, that the in-ground footing had some sand, gravel, or other material covering at the time of the bombing. This is supported by the observation that the granite collar, which was located on top of the footing and was well above the ground, shows good agreement with the calculations.

If, for example, we assume that there were 5 cm of sand or equivalent material on top of the in-ground footing, then it is observed in Figure 10 that the measurements and calculations would agree reasonably well at depths greater than 10 cm.

The measurement at about 8 cm of concrete in Figure 10 appears to continue to suggest a surface chloride exchange problem. It is noted that since the footing was near a walkway at the Torii gate, it is likely that salt may have been used for deicing at that location. Salt used for that purpose is very low in ^{36}Cl and would tend to reduce the $^{36}\text{Cl}/\text{Cl}$ ratio near the surface of the concrete. Also, it would be expected that under those conditions, i.e., where there may be standing concentrated salt water on the surface of the concrete footing, the Cl may penetrate somewhat deeper than in a vertical concrete wall.

Shirakami Shrine (granite core, 487 m from hypocenter). These ^{36}Cl measurement results are plotted in Figure 11 together with the sample-specific DS86 and DS02 calculations. Except for decreased $^{36}\text{Cl}/\text{Cl}$ measured very close to the surface of the core (0-2 cm slice), the measurements and calculations are in agreement. Although the DS86 calculations appear to be consistently higher than the DS02 calculations, both are in reasonably good agreement with the $^{36}\text{Cl}/\text{Cl}$ measurements at depths from 3 cm to more than 40 cm in the core. These results suggest that some chloride exchange may also occur in granite very near the surface, perhaps within the first cm or so. Importantly, the results show that chloride exchange did not affect the 2 to 4 cm slice in this granite core. The details of the modeling calculations performed to account for trees etc. in the vicinity of the Shirakami shrine granite rock are presented in Chapter 8, Part J. It should be noted that aerial photographs of the Shirakami shrine taken prior to the bombing show that there were several trees in the vicinity of the granite rock that was sampled here. These trees were taken into account in the modeling calculations.

Kirin Beer Hall (concrete core, 679 m from hypocenter). The ^{36}Cl measurement results are plotted in Figure 12 together with the sample-specific DS86 and DS02 calculations. Several observations are notable. First, the results show that this building (or at least the part of the wall where this core was obtained) was resurfaced after the bombing. The $^{36}\text{Cl}/\text{Cl}$ ratios near the surface approach background levels. Second, the measurements beyond 5 cm tend to be somewhat lower than the DS86 and DS02 calculations, although the slopes are the same. Third, in order to evaluate the possibility that meteoric chloride could penetrate to large depths in this particular concrete, cement and pebbles were separated and chloride extracted for AMS analysis. The hypothesis being that chloride in, e.g., rain water, may penetrate the porous cement but not the solid pebbles. These results are also plotted in Figure 12 and demonstrate that there is no detectable difference in the measured $^{36}\text{Cl}/\text{Cl}$ between cement and pebbles at depths of 8.5 cm and deeper in concrete. However, at 5.5 cm the difference is significant. At that depth, the measured result for the cement fraction was $4.45 \times 10^{-12} \pm 8.20 \times 10^{-14}$ (SD), and the measured result for the pebble fraction was $7.65 \times 10^{-12} \pm 1.30 \times 10^{-13}$ (SD). It is important to note that these two measurements were performed using the same AMS machine, and both were during the same run, so there should be no inter-machine or inter-run issues. If we compare the background-subtracted result for the pebbles at 5.5 cm with DS02, the measurement is within 28% of the DS02 calculation. Unfortunately, we could not evaluate pebbles in slices closer to the surface, since they were composed of surface cement only.

Activation Measurements for Thermal Neutrons

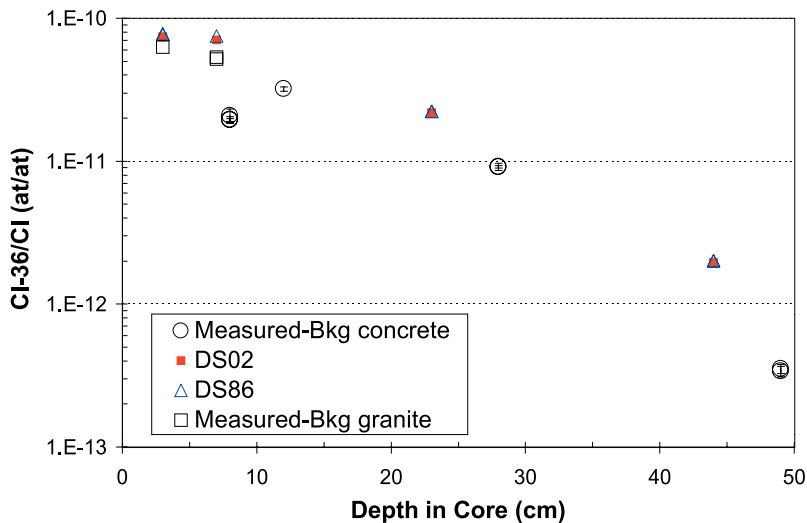


Figure 10. Depth profile in concrete footing and granite collar from the Gokoku Shrine in Hiroshima. [Assumes 5 cm of sand or equivalent material on the surface of the concrete footing.]

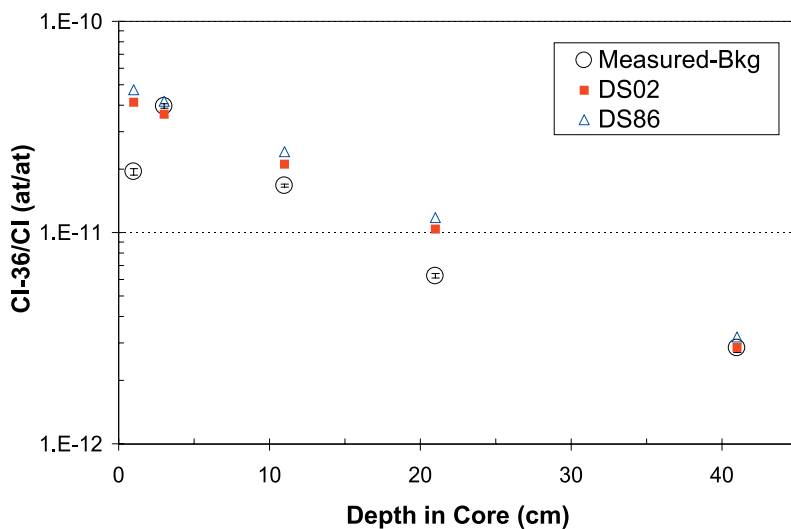


Figure 11. Depth profile in concrete and granite cores from the Shirakami Shrine in Hiroshima.

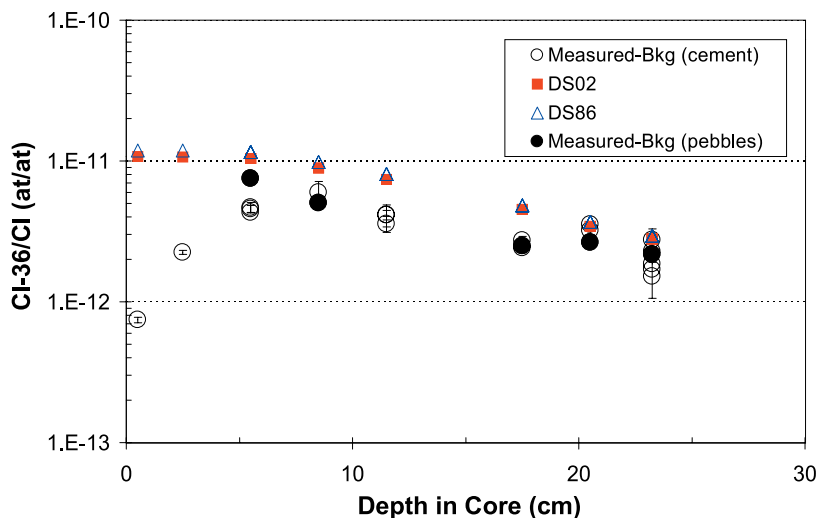


Figure 12. Depth profile in a concrete core from the Kirin Beer Hall in Hiroshima.

As indicated above, it is clear from Figure 12 that the surface of the Kirin Beer Hall wall was modified after the war. The surface of the core that we measured contained tiles. The tiles were therefore put on the wall after the bombing. This means that we do not know how much the wall was modified, i.e., how much may have been removed from or added to the wall during the renovation. However, removing only a few centimeters from the surface of the building is all that would have been required to provide perfect agreement.

Hiroshima City Hall (concrete core, 1,060 m from the hypocenter). The ^{36}Cl measurement results are plotted in Figure 13 together with the sample-specific DS86 and DS02 calculations. It is observed that the agreement between the ^{36}Cl measurements and the calculations is very good. Although the measured $^{36}\text{Cl}/\text{Cl}$ at the surface is somewhat lower than expected (consistent with surface chloride exchange), the measurements and calculations agree from 6.5 cm to almost 50 cm mean depths. It is noted that such a depth profile is a good test for the modeling calculations and provides more information about the incident neutrons than a surface sample alone. As with all of the modeling calculations performed specifically for these samples, the total calculated $^{36}\text{Cl}/\text{Cl}$ was obtained by summing both the $^{35}\text{Cl}(\text{n},\gamma)^{36}\text{Cl}$ and the $^{39}\text{K}(\text{n},\alpha)^{36}\text{Cl}$ reactions. The $^{35}\text{Cl}(\text{n},\gamma)$ is a thermal neutron reaction, while the $^{39}\text{K}(\text{n},\alpha)$ is mostly from fast neutrons. As an example, their relative contributions to total $^{36}\text{Cl}/\text{Cl}$ in the Hiroshima City Hall core as calculated for DS02 are more than 95% $^{35}\text{Cl}(\text{n},\gamma)^{36}\text{Cl}$ and less than 5% $^{39}\text{K}(\text{n},\alpha)^{36}\text{Cl}$.

Red Cross Hospital (concrete cores, ~1,500 m from the hypocenter). The ^{36}Cl measurement results plotted in Figure 14 are for a core taken at 20 m above the ground from the tower of the building at 1,501 m ground range. These measurements are compared with the sample-specific DS86 and DS02 calculations. With the possible exception of the measurement closest to the surface, it is observed that the measurements are in good agreement with the calculations for both DS02 and DS86. It is also observed that at this distance, it appears that we have reached the limit of detection for ^{36}Cl induced in concrete by Hiroshima neutrons. Also shown for comparison,

results for same-sample aliquots measured at the AMS facility in Munich (Chapter 8, Part E) agree with the measurements made here using AMS facilities at LLNL and Purdue. Although not statistically significant, it is noted however that the same-sample Munich measurements do appear to be suggestively lower than those at both LLNL and Purdue.

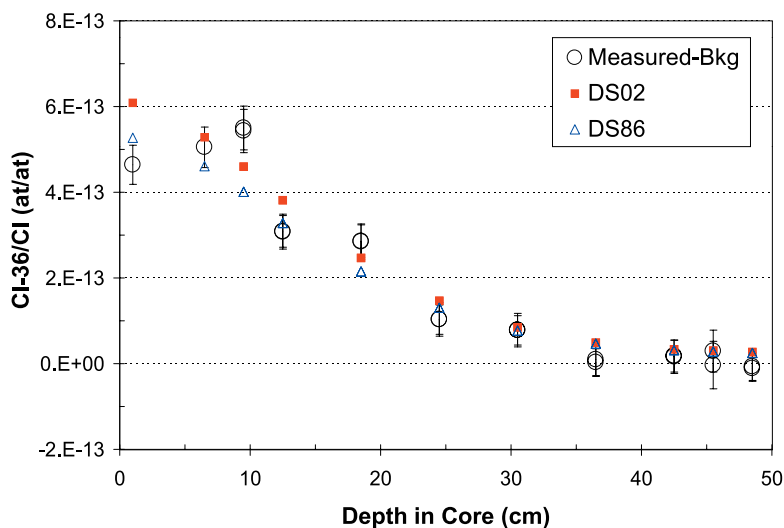


Figure 13. Depth profile in a concrete core from the old Hiroshima City Hall.

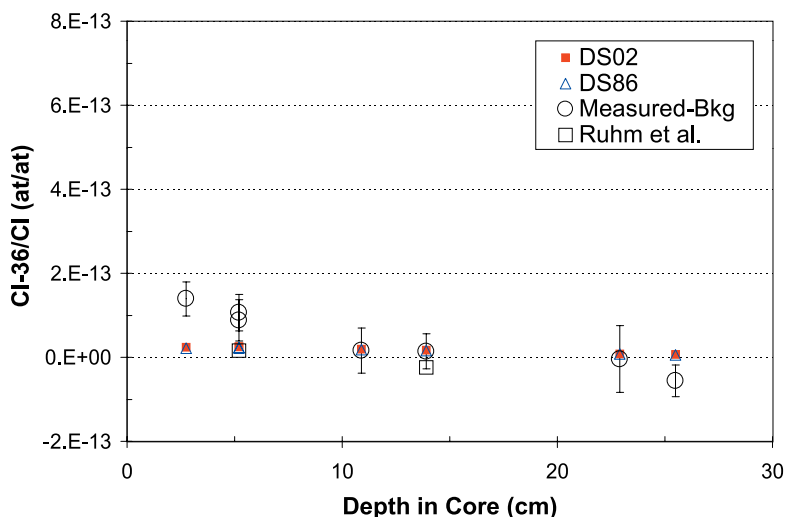


Figure 14. Depth profile in concrete core S-76 obtained at 20 m above ground from the Red Cross Hospital in Hiroshima. The two open squares were measurements (minus our estimated background from Figure 1) made by Rühm and others at the Munich AMS facility in aliquots provided by us and were from the same Cl extraction as the other measurements at the same depth.

A photograph of this Red Cross Hospital core is seen in Figure 15, with the locations marked for the slices to be cut. Note that slices 2 through 10 contain the original concrete wall. Slice 1 is clearly a different type of material, which is on the outside surface of the building. The concrete appears solid and good quality, with normal concentrations of pebbles and cement.



Figure 15. Concrete core S-76 from the Hiroshima Red Cross Hospital. This core was taken at 20 m above ground level from the tower of the building. The locations of the slices are marked on the core, and slice #1 is at the outside surface facing the hypocenter.

The ^{36}Cl results plotted in Figure 16 are for two concrete cores taken at 9 m above ground from another part of the Red Cross Hospital at 1,474 m ground range. These cores were visibly much more porous (lower density concrete) than core S-76 from the tower, and the results exhibit more scatter than those in Figure 14. It may be that the scatter is due to the high porosity of this particular concrete leading to more exchange of chloride with the surface. It is also possible (likely) that the scatter (especially within the first ~10 cm) is caused by the unusually large amount of surface cement on this particular wall, which may be from different sources of materials than the concrete wall itself. It is also noted that this particular concrete had higher sulfur concentration than generally observed, which resulted in some samples not being possible to measure correctly. This is the reason for only plotting the first three data points of core S-59. Given these observations, we believe that the results from cores S-59 and S-60 may be less reliable than those from core S-76, which was composed of much denser concrete, had less sulfur, and much less surface cement. In any case, a detectable bomb-induced depth profile is not observed in these cores. Taken together, the ^{36}Cl measurements in the cores from the Red Cross Hospital are consistent with both DS86 and DS02. The conclusion is that we simply cannot resolve the difference between the bomb-induced ^{36}Cl and the “background” ^{36}Cl at these large distances.

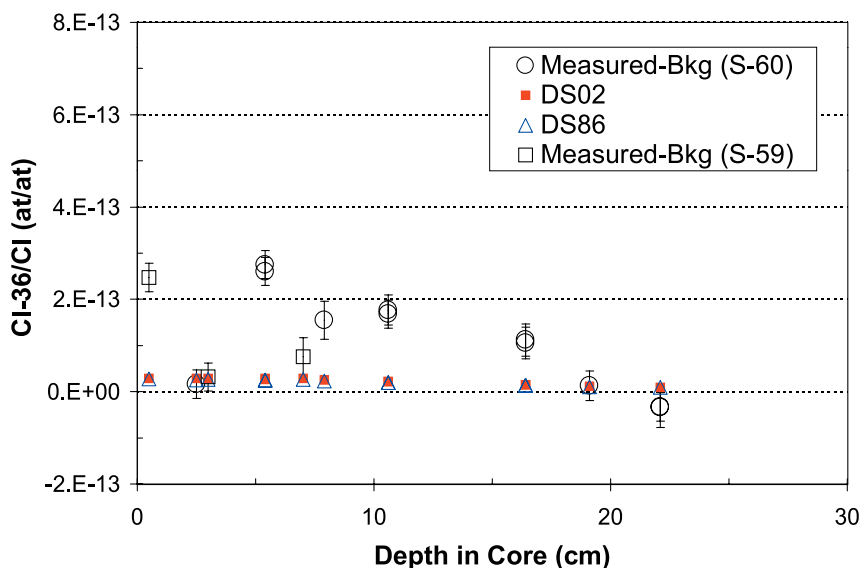


Figure 16. Depth profiles in concrete cores S-59 and S-60 obtained at 9 m above ground from the Red Cross Hospital in Hiroshima.

A photograph of core S-60 is seen in Figure 17. It is observed that this core is of substantially lower quality than core S-76 and much more porous, especially toward the end facing the hypocenter (indicated by arrow drawn on the core).

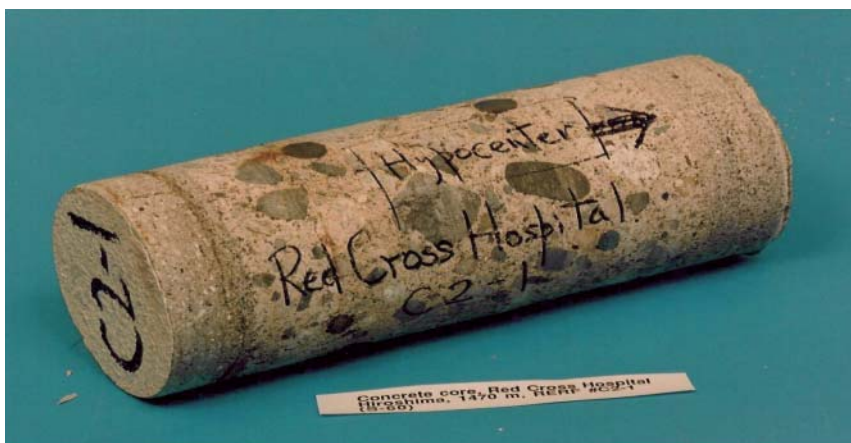


Figure 17. Concrete core S-60 from the Hiroshima Red Cross Hospital. This core was taken at 9 m above ground level from a concrete wall of the building. The outside surface facing the hypocenter (marked by arrow) is very porous with no covering such as tiles or other protective surface material.

Hiroshima Postal Savings Bureau (concrete core, 1,591 m from the hypocenter). The ^{36}Cl measurement results for this core are plotted in Figure 18 together with the sample-specific DS86 and DS02 calculations. Because of the high $^{36}\text{Cl}/\text{Cl}$ observed in the surface cement (which included surface tiles and grout), we separated cement and pebbles to assess whether mobile “contaminants” on the surface may have penetrated deeper into the concrete wall. Because the exterior walls of the Postal Savings Bureau building were covered with tiles, it would be expected that the interior of the walls should be largely protected from meteoric contaminants. The results in Figure 18 would tend to support this conclusion. Except for the two measurements made in the surface sample (which are consistent with meteoric surface contamination or high $^{36}\text{Cl}/\text{Cl}$ ratios inherent in the tile/grout material), the results for this core are also consistent with both DS86 and DS02 calculations. There is no indication of a detectable bomb-induced depth profile.

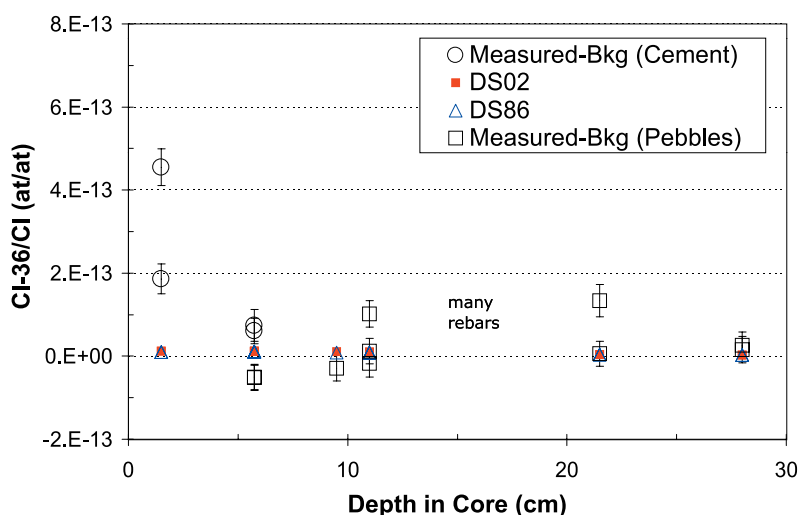


Figure 18. Depth profile in concrete core obtained from the Postal Savings Bureau in Hiroshima. Note that there was an unusual number of steel reinforcement bars between 13 and 20 cm depth.

^{41}Ca Measurements

In addition to ^{36}Cl measurements in concrete and granite, we have also made a few confirmatory ^{41}Ca measurements in three of the same samples (i.e., granite from the Motoyasu Bridge, concrete from the Hiroshima Bank, and concrete from the Kirin Beer Hall). Calcium-41 is produced by thermal neutrons via the reaction, $^{40}\text{Ca}(n,\gamma)^{41}\text{Ca}$. The half-life of ^{41}Ca is 140,000 years. In contrast to chlorine, calcium is much less soluble and should therefore not exhibit significant surface mobility. The results are plotted in Figure 19 together with sample-specific DS02 calculations. It is seen that the ^{41}Ca results are in good agreement with DS02 at the distances where measurements have been made. The cross section for $^{40}\text{Ca}(n,\gamma)^{41}\text{Ca}$ is only about 1% of that for ^{36}Cl , and therefore the limit of detection is reached at a substantially shorter

distance. The mean measured-to-calculated ratio for the two closest distances is 1.01 ± 0.25 , clearly not different from unity. For the Motoyasu Bridge granite sample (130 m ground range), the M/C based on ^{41}Ca is 1.20 ± 0.25 . For comparison, the ^{36}Cl results for the same sample have M/C of 0.92 ± 0.07 . For the Hiroshima Bank concrete sample (257 m ground range), the M/C based on ^{41}Ca is 0.96 ± 0.26 . For comparison, the ^{36}Cl results for the Hiroshima Bank sample is 0.58 ± 0.02 , significantly lower than the equivalent ^{41}Ca measured in the same sample. In contrast, the M/C results for ^{41}Ca and ^{36}Cl in the granite sample from the Motoyasu Bridge do not differ significantly.

These ^{41}Ca results are consistent with the observation that the solubility of meteoric Cl can reduce somewhat the $^{36}\text{Cl}/\text{Cl}$ ratio in surface concrete from Hiroshima at these distances. They also support the observation that Cl is less mobile in granite than in concrete.

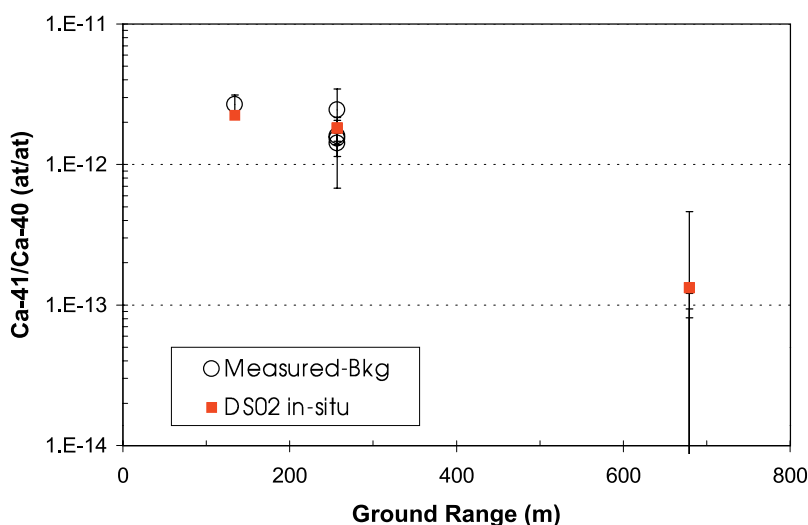


Figure 19. ^{41}Ca measured in selected concrete and granite samples from Hiroshima. The sample locations are: Motoyasu Bridge (130 m ground range); Hiroshima Bank (257 m ground range); Kirin Beer Hall (679 m ground range).

^{36}Cl Measurements in Samples from Nagasaki

The majority of the measurement results for Nagasaki were published in Straume et al. (1994). However, there have been some additional ^{36}Cl measurements made in Nagasaki since that publication, and they are included here and discussed for completeness. Also, new comparisons are made with DS02 calculations.

Materials and Methods

Samples. The samples from Nagasaki were concrete cores obtained from reinforced concrete buildings known to have been present at the time of the atomic bomb explosion in 1945. Cores

(10-cm diameter, typically ~30-cm long) were obtained from walls in line-of-sight with the bomb explosion, and also from shielded parts of the same buildings. The line-of-sight cores were used to measure the bomb-induced ^{36}Cl , and the shielded cores were used to measure the pre-bomb ^{36}Cl levels in the same or similar concrete. Table A19 of Appendix A lists information pertinent to each in line-of-sight core from Nagasaki.

The availability of suitable concrete samples from Nagasaki was very limited. In contrast to Hiroshima, few buildings remain in Nagasaki that were exposed to the atomic bomb in 1945. It is fortunate that excellent concrete cores were obtained from four structures in Nagasaki (Nagasaki University Hospital, Mitsubishi Steel & Arms Works, Fuchi Middle High School, and the Konpirasan mountain gun emplacement). These concrete structures span distances of importance to the survivor dosimetry, i.e., from 653 m to 1,582 m ground range.

The elemental composition of each core was determined. Major elements, except oxygen, carbon, and hydrogen, were determined by inductively-coupled plasma atomic emission spectroscopy (ICP-AES). Carbon and hydrogen were determined by combustion analysis. Oxygen was determined by mass-balance analysis, and trace elements were determined by ICP-mass spectrometry. The elemental compositions for the Nagasaki cores were provided in Straume et al. (1994).

Sample Preparation. The concrete cores were cut into approximately 3-cm-thick slices. The first slice contained the cement-like material on the outside of the wall, and, because of the possibility of surface contamination or resurfacing of the building after the war, the first slice was not used to determine bomb-induced ^{36}Cl activation. Rather, the second or third slice, whichever was visually identified to be part of the actual reinforced concrete wall, was used for that purpose. The concrete slices were ground and chloride extracted as described in Straume et al. (1994).

Accelerator Mass Spectrometry. As with Hiroshima, the measurements in Nagasaki samples were made by AMS. For information concerning AMS, see Hiroshima Measurements section.

Calculations for Nagasaki. To compare measured ^{36}Cl activation with calculations, the bomb-induced $^{36}\text{Cl}/\text{Cl}$ ratios in the Nagasaki samples were calculated using both the DS86 and DS02 methodologies. The computational methods and neutron cross sections used are described in Chapter 8, Part J.

Nagasaki Results and Discussion

Results for ^{36}Cl activation in Nagasaki samples measured using AMS are listed in Table A20 of Appendix A. Twenty line-of-sight measurements were made, seven at 653 m, six at 1,075 m, five at 1,156 m, and two at 1,582 m. Each measurement result has an associated standard deviation (SD) that was based on both analytical uncertainties associated with the AMS machine and the contributions from background subtraction.

The ^{36}Cl results listed in Table A20 are plotted in Figure 20. In this case, the measured (gross) values are plotted. It is observed that the measurements without background subtraction appear to level-off at about 1×10^{-13} $^{36}\text{Cl}/\text{Cl}$, which is consistent with a considerable body of background data that have now been obtained from both Hiroshima and Nagasaki (Figure 1).

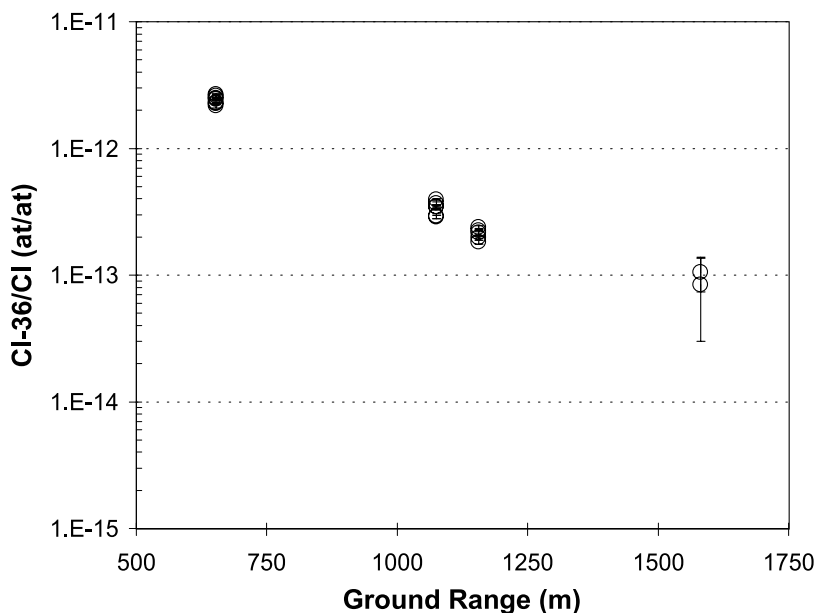


Figure 20. Measurements of ^{36}Cl in Nagasaki line-of-sight concrete samples. Surface cement was excluded from these measurements.

When the background is subtracted from the measurements, the bomb-induced $^{36}\text{Cl}/\text{Cl}$ ratios decrease exponentially and are consistent with the DS02 calculations (Figure 21).

In addition to line-of-sight concrete samples, two concrete cores were also analyzed in Nagasaki. One core was from the Nagasaki University Hospital at 653 m ground range, and the other was from the Konpirasan mountain gun emplacement at 1,582 m ground range. The $^{36}\text{Cl}/\text{Cl}$ depth profile in the Nagasaki University Hospital core was checked in 1993 by measuring a slice taken at 2 to 5 cm and another at 30 to 33.5 cm depth. The purpose was to test the measured depth profile against the calculation using DS86 (Straume et al. 1994) and now against DS02. The measured minus background $^{36}\text{Cl}/\text{Cl}$ results from these two depths were $2.29 (\pm 0.18) \times 10^{-12}$ and $6.22 (\pm 0.2) \times 10^{-13}$, respectively. This compares with the DS02 calculated values of 2.74×10^{-12} and 4.08×10^{-13} . The comparisons for DS86 calculations at these depths are 3.70×10^{-12} and 5.35×10^{-13} . It appears that DS02 calculations substantially improved the line-of-sight (i.e., 2-to-5 cm depth) comparison at 653 m ground range in Nagasaki. It should be pointed out that the calculated values at 30-to-33.5 cm depth for both DS02 and DS86 are within the range of variation possible by reasonable assumptions in the concentrations of poisons, water content, density, etc.

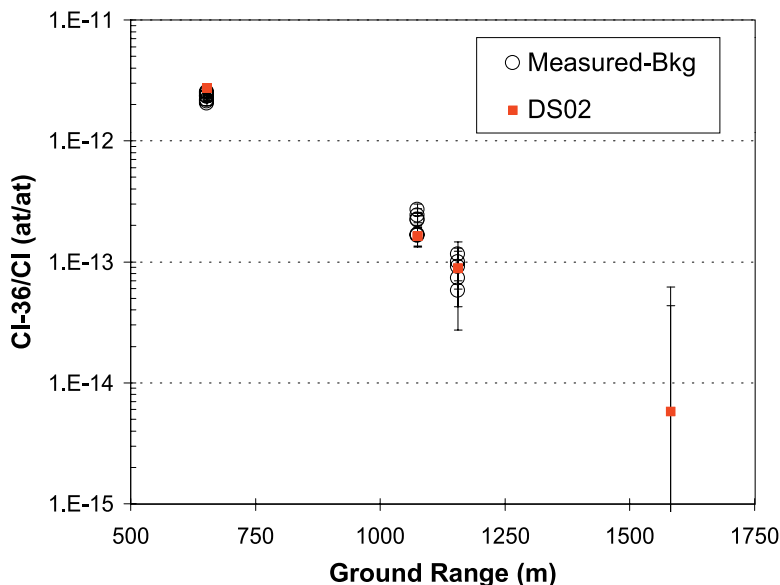


Figure 21. Measurements and DS02 calculations compared for ^{36}Cl in Nagasaki concrete samples. Surface cement was excluded from these measurements and a background of 1.24×10^{-13} was subtracted from the measured values.

The core from the Konpirasan gun emplacement was at a distance from the hypocenter sufficiently large to evaluate background ^{36}Cl in Nagasaki concrete, and also provides additional information on the $^{36}\text{Cl}/\text{Cl}$ ratios in essentially non-bomb exposed surface cement. It is observed in Figure 22 that the ^{36}Cl in surface cement is higher than in the interior concrete and that the interior of the concrete wall is consistent with a background of about 1×10^{-13} $^{36}\text{Cl}/\text{Cl}$. Again, this is consistent with the substantial background data now available for both concretes and granites in Hiroshima and Nagasaki.

To compare further the ^{36}Cl -activation measurements and calculations in Nagasaki, the measured bomb-induced $^{36}\text{Cl}/\text{Cl}$ ratios were divided by the ratios calculated specifically for the same samples using DS86 and DS02. Results are provided in Table A21 of Appendix A. If neutron measurements and calculations are correct in the Nagasaki dosimetry, the M/C ratios for $^{36}\text{Cl}/\text{Cl}$ should be consistent with unity. The mean M/C ratios for all combined line-of-sight measurements in Nagasaki are 1.04 ± 0.25 when compared with DS02 calculations and 0.84 ± 0.25 when compared with DS86 calculations (i.e., using pre 1993 delayed neutrons and cross sections). The M/C for DS02 is clearly not significantly different from 1.0. However, the M/C for DS86 is significantly below unity at the 653 m distance. It should be noted, however, that the “DS86” used for these comparisons did not include the revisions made in 1993 to the Nagasaki calculations, i.e., updated neutron cross sections (ENDF/B-6.2), more energy groups, delayed neutron source extended to higher energies, and two-dimensional treatment of the delayed radiation. Those adjustments were included in Straume et al. (1994) and resulted in values similar to DS02, and hence a good fit to the ^{36}Cl measurements in Nagasaki.

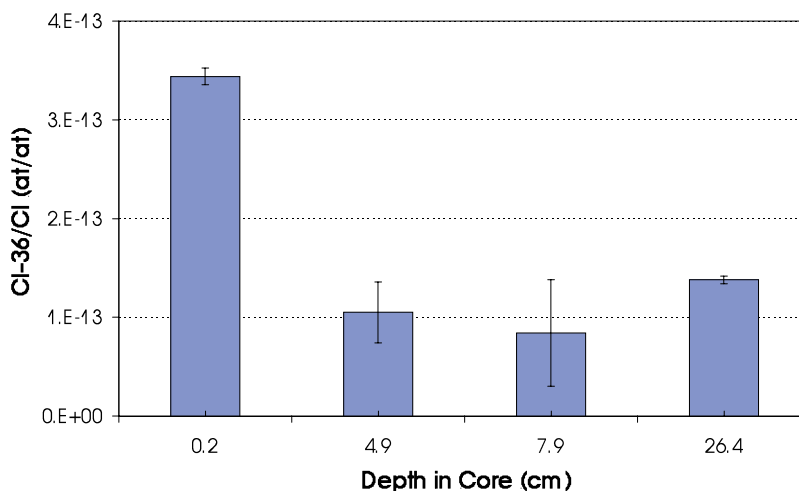


Figure 22. Depth profile of $^{36}\text{Cl}/\text{Cl}$ measured in concrete core from the Konpirasan Mountain gun emplacement at 1,582 m ground range in Nagasaki.

Conclusions

Measurements of ^{36}Cl in granite and concrete (excluding the surface in concrete) in samples from Hiroshima and Nagasaki are consistent with DS02 from near the hypocenter to distances where $^{36}\text{Cl}/\text{Cl}$ ratios become indistinguishable from background. The ^{36}Cl background has only a minor effect on the results at distances less than about 1 km from the hypocenter, and therefore uncertainties in the background could not alter the agreement observed with DS02 at those distances.

The core profile measurements suggest that meteoric chloride can penetrate porous cement and affect the $^{36}\text{Cl}/\text{Cl}$ ratio near the surface. The results also show that granite is less affected by this than cement.

The high M/C ratios for ^{36}Cl beyond 1,400 m in Hiroshima suggested previously (Straume et al. 1992) resulted from the use of surface cement, which can have a higher background than deeper concrete. Based on the extensive work presented here, it is now clear that those high surface measurements were not produced by bomb neutrons. Similarly elevated ^{36}Cl levels are observed in surface cement from both Hiroshima and Nagasaki, even at distances well beyond the reach of significant bomb neutrons.

Avoiding surface cement, the measurements in concrete cores from Nagasaki agree well with DS02. It has been shown previously (Straume et al. 1994) that DS86 updated with 1993 delayed neutrons and cross sections also agreed well with the ^{36}Cl measurements in Nagasaki.

Acknowledgment

We thank the following organizations for supporting this work: the U.S. Department of Energy (grant #DEFG0300ER62963; contract #DEFC0397SF21354), the U.S. National Academy of Sciences (grant #E215099), the U.S. Army Surgeon General's Office (C. Curling), and the Defense Nuclear Agency (R. W. Young). Portions of this work were performed under the auspices of the U.S. Department of Energy by the University of California, Lawrence Livermore National Laboratory under contract W-7405-Eng-48. We also thank R. Finkel and colleagues of the AMS facility at LLNL and D. Elmore, P. Sharma, and colleagues of the AMS facilities at Purdue and Rochester.

References

- Dep, L.; Elmore, D.; Fabryka-Martin, J.; Masarik, J.; Reedy, R. C. "Production Rate Systematics of In-Situ-Produced Cosmogenic Nucleides in Terrestrial Rocks: Monte Carlo Approach of Investigating $^{35}\text{Cl}(n,\gamma)^{36}\text{Cl}$." *Nuc. Instr. Meth. B92*: 321-325; 1994.
- Elmore, D.; Tubbs, L. E.; Newman, D.; Ma, X. Z.; Finkel, R.; Nishiizumi, K.; Beer, J.; Oeschgar, H.; Andrea, M. "The ^{36}Cl Bomb Pulse Measured in a Shallow Ice Core from Dye-3, Greenland." *Nature* 300: 735-737; 1982.
- Elmore, D.; Phillips, F. M. "Accelerator Mass Spectrometry for Measurement of Long-Lived Radioisotopes." *Science* 236: 543-550; 1987.
- Haberstock, G.; Heinzl, J.; Korschinek, G.; Morinaga, H.; Nolte, E.; Ratzinger, U.; Kato, K.; Wolf, M. "Accelerator Mass Spectrometry with Fully Stripped ^{36}Cl Ions." *Radiocarbon* 28: 204-210; 1986.
- Hainsworth, L. J.; Mignerey, A. C.; Helz, G. R.; Sharma, P.; Kubik, P. W. "Modern ^{36}Cl Dggeposition in Southern Maryland, U.S.A." *Nuc. Instr. Meth. Phys. Res. B92*: 345-349; 1994.
- Ingersoll, D. T.; Roussin, R. W.; Fu, C. Y.; White, J. E. *DABLE69: A Broad-Group Neutron/Photon Cross-Section Library for Defense Nuclear Applications*. Oak Ridge, Tennessee: Oak Ridge National Laboratory; ORNL/TM-10568; 1989.
- Johnson, J. O.; ed. *A User's Manual for MASH 1.0—A Monte Carlo Adjoint Shielding Code System*. Oak Ridge, Tennessee: Oak Ridge National Laboratory, ORNL/TM-11778; 1999.
- McVane, V.; Dunford, C. L.; Rose, P. F.; eds. *ENDF-102: Data Formats and Procedures for the Evaluated Nuclear Data File ENDF-6*. Upton, New York: Brookhaven National Laboratory; BNL-NCS-44945 Revised; 1995.
- Paulsson-Tralla, J.; Silfwerbrand, J. "Estimation of Chloride Ingress in Uncracked and Cracked Concrete Using Measured Surface Concentrations." *ACI Materials Journal* 99: 27-36; 2002.
- Phillips, F. M. "Chlorine-36." In: *Environmental Tracers in Subsurface Hydrology*, pp. 299-348 (Cook, P. G.; Herczeg, A. L.; eds.). Boston: Massachusetts; Kluwer Academic Publishers; 1999.
- Roesch, W. C.; ed. *US-Japan Joint Reassessment of Atomic Bomb Radiation Dosimetry in Hiroshima and Nagasaki, Final Report*. Hiroshima, Japan: Radiation Effects Research Foundation; 1987.
- Schaeffer, O. A.; Thompson, S. O.; Lark, N. L. "Chlorine-36 Radioactivity in Rain." *J. Geophys. Res.* 65: 4013-4016; 1960.

- Sharma, P.; Kubik, P. W.; Fehn, U.; Gove, G. E.; Nishizumi, K.; Elmore, D. "Development of ^{36}Cl Standards for AMS." *Nucl. Instr. Meth. Phys. Res.* B52: 410-415; 1990.
- Shizuma, K.; Iwatani, K.; Hasai, H.; Hoshi, M.; Oka, T.; Morishima, H. "Residual ^{152}Eu and ^{60}Co Activities Induced by Neutrons from the Hiroshima Atomic Bomb." *Health Phys.* 65: 272; 1993.
- Shizuma, K.; Iwatani, K.; Hasai, H.; Hoshi, M.; Oka, T. "Eu Depth Profiles in Granite and Concrete Cores Exposed to the Hiroshima Atomic Bomb." *Health Phys.* 72: 848-855; 1997.
- Straume, T.; Finkel, R. C.; Eddy, D.; Kubik, P. W.; Gove, H. E.; Sharma, P.; Fujita, S.; Hoshi, M. "Use of Accelerator Mass Spectrometry in the Dosimetry of Hiroshima Neutrons." *Nucl. Instr. Meth. Phys. Res.* B52: 552-556; 1990.
- Straume, T.; Egbert, S. D.; Woolson, W. A.; Finkel, R. C.; Kubik, P. W.; Gove, H. E.; Sharma, P.; Hoshi, M. "Neutron Discrepancies in the DS86 Hiroshima Dosimetry System." *Health Phys.* 63: 421; 1992.
- Straume, T.; Harris, L. J.; Marchetti, A. A.; Egbert, S. D. "Neutrons Confirmed in Nagasaki and at the Army Pulsed Radiation Facility: Implications for Hiroshima." *Radiat. Res.* 138: 193-200; 1994.
- Synal, H. A.; Beer, J.; Bonani, G.; Suter, M.; Wolfli, W. "Atmospheric Transport of Bomb-Produced ^{36}Cl ." *Nucl. Instr. Meth. Phys. Res.* B52: 483-488; 1990.
- White, J. E.; Ingersoll, D. T.; Wright, R. Q.; Hunter, H. T.; Slater, C. O.; Greene, M. N.; MacFarlane, R. E.; Roussin, R. W. *Production and Testing of the Revised VITAMIN-B Fine-Group and the BUGLE-96 Broad Group Neutron/Photon Cross-Section Libraries Derived from ENDF/B-VI.3 Nuclear Data*. Oak Ridge, Tennessee: Oak Ridge National Laboratory; ORNL/TM-6795/R1; April 2000.
- Zerle, L.; Faestermann, T.; Knie, K.; Korschinek, G.; Nolte, E. "The ^{41}Ca Bomb Pulse and Atmospheric Transport of Radionuclides." *J. Geophys. Res.* 102: 517-527; 1997.

Appendix A

This appendix contains results of ^{36}Cl measurements and sample-specific calculations.

Table A1. Locations and types of sample materials from Hiroshima measured for ^{36}Cl in the U.S.

Sample location	Sample material	DS86 ground range (m)	DS02 ground range (m)
Motoyasu Bridge	Granite core	145	134
Motoyasu Bridge	Granite core	139	128
Hiroshima Bank	Concrete sample	242	257
Aioi Bridge	Granite sample	270	257
Gokoku Shrine	Concrete core	394	388
Gokoku Shrine	Granite core	394	388
Shirakami Shrine	Granite core	478	487
Shirakami Fence	Granite sample	496	504
Chugoku Electric Co.	Concrete sample	664	670
Kirin Beer Hall	Concrete core	664	679
Myochoji	Granite sample	654	639
Old Prefecture Office	Granite sample	881	877
Old Prefecture Office	Granite sample	881	877
Honkeiji	Granite sample	893	896
Enryuuj	Granite sample	912	925
Shingyoji	Granite sample	927	915
Hiroshima City Hall	Concrete core	1055	1060
Kozenji	Granite sample	1163	1177
HU Elementary School	Concrete core	1269	1277
Ono Oil Shop	Granite sample	1292	1291
Teishin Hospital	Concrete core	1368	1375
HU, Main Bldg.	Surface cement	1378	1386
HU Radioisotope	Concrete core	1458	1466
Red Cross Hospital	Concrete core	1470	1474
Red Cross Hospital	Concrete core	1470	1474
Red Cross Hospital	Concrete core	1496	1501
Postal Savings	Concrete core	1585	1591
Postal Savings	Concrete core	1594	1600
Misasa Bank	Concrete core	1689	1682
Commercial High School	Concrete core	2864	2858
Senngyoji	Granite sample	Highly shielded	Highly shielded
Kannonji	Granite sample	Highly shielded	Highly shielded

Table A2. Near surface measurements in granite samples from Hiroshima

Sample location	DS86 ground range (m)	DS02 ground range (m)	Mean depth (cm)	Measured Cl-36/Cl	Measured-bkg Cl-36/Cl	SD Cl-36/Cl	DS86 Cl-36/Cl	DS02 Cl-36/Cl
Motoyasu Bridge	139	128	1	1.18E-10	1.18E-10	1.17E-12	1.83E-10	1.62E-10
Motoyasu Bridge	139	128	3	1.42E-10	1.42E-10	1.95E-12	1.66E-10	1.46E-10
Motoyasu Bridge	139	128	7	1.21E-10	1.21E-10	2.03E-12	1.37E-10	1.20E-10
Motoyasu Bridge	145	134	1	1.46E-10	1.46E-10	8.51E-12	2.01E-10	1.81E-10
Motoyasu Bridge	145	134	4	1.69E-10	1.69E-10	1.88E-12	1.94E-10	1.73E-10
Motoyasu Bridge	145	134	1	1.64E-10	1.64E-10	1.53E-12	2.01E-10	1.81E-10
Motoyasu Bridge	145	134	4	1.71E-10	1.71E-10	2.13E-12	1.94E-10	1.73E-10
Aioi Bridge ^a	270	257	1.5	9.00E-11	8.98E-11	3.38E-12	1.30E-10	1.26E-10
Gokoku Shrine	394	388	3	6.29E-11	6.28E-11	9.58E-13	6.14E-11	5.97E-11
Gokoku Shrine	394	388	7	5.20E-11	5.19E-11	7.91E-13	5.25E-11	5.06E-11
Gokoku Shrine	394	388	7	5.37E-11	5.36E-11	1.06E-12	5.25E-11	5.06E-11
Shirakami Shrine	478	487	1	1.94E-11	1.93E-11	6.68E-13	4.75E-11	4.13E-11
Shirakami Shrine	478	487	3	3.97E-11	3.96E-11	9.49E-13	4.18E-11	3.64E-11
Shirakami fence	496	504	1	2.19E-11	2.18E-11	4.00E-13	3.26E-11	3.02E-11
Shirakami fence	496	504	1	2.11E-11	2.10E-11	9.15E-13	3.26E-11	3.02E-11
Myochoji	654	639	1	9.59E-12	9.47E-12	3.63E-13	9.99E-12	1.17E-11
Myochoji	654	639	1	9.85E-12	9.73E-12	3.15E-13	9.99E-12	1.17E-11
Old Prefecture	881	877	2.5	4.14E-12	4.02E-12	3.72E-13	1.60E-12	1.95E-12
Old Prefecture	881	877	2.5	4.15E-12	4.03E-12	8.11E-14	1.60E-12	1.95E-12
Old Prefecture	881	877	2.5	2.37E-12	2.25E-12	1.30E-13	1.60E-12	1.95E-12
Honkeinji	893	896	1	1.39E-12	1.27E-12	4.93E-14	1.45E-12	1.68E-12
Honkeinji	893	896	1	1.38E-12	1.26E-12	5.36E-14	1.45E-12	1.68E-12
Enryuuj	912	925	2.5	1.20E-12	1.08E-12	8.03E-14	1.25E-12	1.34E-12
Enryuuj	912	925	2.5	1.38E-12	1.26E-12	5.48E-14	1.25E-12	1.34E-12
Shingyoji	927	915	2.5	1.32E-12	1.20E-12	1.02E-13	1.11E-12	1.45E-12
Shingyoji	927	915	2.5	1.32E-12	1.20E-12	4.36E-14	1.11E-12	1.45E-12
Kozenji	1163	1177	1	4.52E-13	3.28E-13	4.45E-14	1.71E-13	1.94E-13
Kozenji	1163	1177	1	4.29E-13	3.05E-13	3.56E-14	1.71E-13	1.94E-13
Ono Oil Shop	1292	1291	7.5	1.51E-13	2.70E-14	3.27E-14	5.72E-14	7.07E-14
Sennyoji	BG	BKG	2.5	1.85E-13		5.07E-14		
Sennyoji	BG	BKG	2.5	1.85E-13		2.60E-14		
Kannonji	BG	BKG	2.5	1.80E-13		2.78E-14		
Kannonji	BG	BKG	2.5	1.68E-13		1.05E-14		

^aFrom Straume et al. 1994.

Table A3. ^{36}Cl measurements in granite samples from the Motoyasu Bridge

Mean depth (cm)	DS86 ground range (m)	DS02 ground range (m)	Measured Cl-36/Cl	Measured-bkg Cl-36/Cl	SD Cl-36/Cl	DS86 Cl-36/Cl	DS02 Cl-36/Cl
1	145	134	1.46E-10	1.46E-10	8.51E-12	2.01E-10	1.81E-10
4	145	134	1.69E-10	1.69E-10	1.88E-12	1.94E-10	1.73E-10
1	145	134	1.64E-10	1.64E-10	1.53E-12	2.01E-10	1.81E-10
4	145	134	1.71E-10	1.71E-10	2.13E-12	1.94E-10	1.73E-10
1	139	128	1.18E-10	1.18E-10	1.17E-12	1.83E-10	1.62E-10
3	139	128	1.42E-10	1.42E-10	1.95E-12	1.66E-10	1.46E-10
7	139	128	1.21E-10	1.21E-10	2.03E-12	1.37E-10	1.20E-10
9	139	128	9.17E-11	9.16E-11	1.07E-12	1.25E-10	1.09E-10
11	139	128	9.16E-11	9.15E-11	1.29E-12	1.14E-10	9.99E-11
21	139	128	5.84E-11	5.83E-11	8.74E-13	7.41E-11	6.43E-11
21	139	128	5.54E-11	5.53E-11	1.57E-12	7.41E-11	6.43E-11
31	139	128	4.30E-11	4.29E-11	8.57E-12	5.64E-11	4.80E-11
31	139	128	4.81E-11	4.80E-11	6.54E-13	5.64E-11	4.80E-11

Table A4. ^{36}Cl measurements in samples from the Gokoku Shrine

Sample material	Mean depth (cm)	DS86 ground range (m)	DS02 ground range (m)	Measured	Measured-bkg Cl-36/Cl	SD Cl-36/Cl	DS86 Cl-36/Cl	DS02 Cl-36/Cl
Concrete	3	394	388	2.09E-11	2.08E-11	2.40E-12	7.75E-11	7.40E-11
Concrete	3	394	388	1.97E-11	1.96E-11	8.29E-13	7.75E-11	7.40E-11
Concrete	3	394	388	1.95E-11	1.94E-11	4.61E-13	7.75E-11	7.40E-11
Concrete	7	394	388	3.21E-11	3.20E-11	1.00E-12	7.50E-11	7.04E-11
Concrete	23	394	388	9.26E-12	9.14E-12	5.02E-13	2.22E-11	2.19E-11
Concrete	23	394	388	9.22E-12	9.10E-12	1.77E-13	2.22E-11	2.19E-11
Concrete	44	394	388	4.76E-13	3.52E-13	4.00E-14	2.02E-12	1.95E-12
Concrete	44	394	388	4.63E-13	3.39E-13	4.14E-14	2.02E-12	1.95E-12
Granite	3	394	388	6.29E-11	6.28E-11	9.58E-13	6.14E-11	5.97E-11
Granite	7	394	388	5.20E-11	5.19E-11	7.91E-13	5.25E-11	5.06E-11
Granite	7	394	388	5.37E-11	5.36E-11	1.06E-12	5.25E-11	5.06E-11

Table A5. ^{36}Cl measurements in granite samples from the Shirakami Shrine

Mean depth (cm)	DS86 ground range (m)	DS02 ground range (m)	Measured Cl-36/Cl	Measured-bkg Cl-36/Cl	SD Cl-36/Cl	DS86 Cl-36/Cl	DS02 Cl-36/Cl
1	496	504	2.19E-11	2.18E-11	4.00E-13	3.26E-11	3.02E-11
1	496	504	2.11E-11	2.10E-11	9.15E-13	3.26E-11	3.02E-11
1	478	487	1.94E-11	1.93E-11	6.68E-13	4.75E-11	4.13E-11
3	478	487	3.97E-11	3.96E-11	9.49E-13	4.18E-11	3.64E-11
11	478	487	1.67E-11	1.66E-11	3.02E-13	2.41E-11	2.10E-11
21	478	487	6.23E-12	6.11E-12	1.56E-13	1.18E-11	1.04E-11
41	478	487	2.84E-12	2.72E-12	1.30E-13	3.20E-12	2.86E-12

Table A6. ^{36}Cl measurements in concrete samples from the Kirin Beer Hall^a

Mean depth (cm)	DS86 ground range (m)	DS02 ground range (m)	Measured Cl-36/Cl	Measured-bkg Cl-36/Cl	SD Cl-36/Cl	DS86 Cl-36/Cl	DS02 Cl-36/Cl
5.5	664	679	4.70E-12	4.58E-12	2.52E-13	1.16E-11	1.04E-11
5.5	664	679	4.81E-12	4.69E-12	4.05E-13	1.16E-11	1.04E-11
8.5	664	679	6.09E-12	5.97E-12	1.20E-12	9.86E-12	8.94E-12
11.5	664	679	4.26E-12	4.14E-12	3.25E-13	8.08E-12	7.41E-12
11.5	664	679	3.70E-12	3.58E-12	4.64E-13	8.08E-12	7.41E-12
11.5	664	679	4.25E-12	4.13E-12	7.34E-13	8.08E-12	7.41E-12
17.5	664	679	2.53E-12	2.41E-12	1.79E-13	4.85E-12	4.51E-12
17.5	664	679	2.85E-12	2.73E-12	1.82E-13	4.85E-12	4.51E-12
20.5	664	679	3.68E-12	3.56E-12	1.32E-13	3.69E-12	3.43E-12
20.5	664	679	3.34E-12	3.22E-12	2.07E-13	3.69E-12	3.43E-12
23.25	664	679	1.99E-12	1.87E-12	8.06E-13	2.93E-12	2.79E-12
23.25	664	679	2.87E-12	2.75E-12	5.49E-13	2.93E-12	2.79E-12
23.25	664	679	2.40E-12	2.28E-12	3.65E-13	2.93E-12	2.79E-12

^aMeasured using the Purdue AMS machine.